

TORQUE AND SPEED FLUCTUATION ON POLYMER PROCESSING LARGE VOLUME KNEADER

*Daniel U. Witte
LIST USA Incorporation
Charlotte, NC 28217-2809*

Abstract

Large volume kneaders are designed to handle highly viscous polymer processing. The unitary operations can be compounding, polymerizations, devolatilization or drying. Depending on the polymer viscosity in the kneader, the interaction of kneading elements induce a torque and force evolution on the shaft over one revolution. Since the torque load depends on the polymer amount and viscosity over the machine length, information about process data, shaft transport and helix angle have to be considered while superimposing the individual load distribution of shaft segments. Torque fluctuations lead to hydraulic drive system pressure fluctuations, which can lead to shaft speed fluctuations due to the hydraulic oil compressibility. The shaft inertia may amplify torque fluctuations on the drive shaft connection. These fluctuations were measured on lab and industrial scale kneaders. A three-dimensional model is presented, which allows accurate assessment of the mechanical design of the shaft and other kneader components.

Introduction

Large volume viscosity kneaders have been used for thermal processing of a broad range of viscous and crust-forming materials for 30 years. Typical behavior of these processes are that a liquid feed material is introduced into the kneader, which is processed through an intermediary pasty, viscous phase to a free flowing material. Most common are 2 types of applications of this kind (see figure 1):

- A mixture of a solvent and a suspended solid is fed into the kneader. The kneader's jacket and shaft are heated and the solvent evaporates under vacuum conditions. Off-gases are extracted through a dome and condensed. The condensate is the product to be reused in this case. With increasing solid content the mixture becomes more viscous and finally turns into a dry free flowing material exempt of solvent, which is discharged through a lock system.

- A liquid reactant (e.g. a monomer) is introduced into the feed zone of the kneader and heated. The feed material reacts into another chemical substance (e.g. a polymer) and the rheological behavior of the reactive mixture changes, becoming more and more viscous with increasing conversion and eventually turns into a free flowing granular material.

In these examples the viscous intermediary phase is limited to a short portion of the kneader length. The induced torque on the shaft is a function of the induced shear and drag forces between the viscous product and the elements. These forces fluctuate over a shaft rotation because the product will distribute itself according to the force interactions. The specific product location will depend only to little extent on gravity since the induced shear and drag forces are much greater than the gravity forces. Product lumps can be observed before each kneading elements (See figure 2).

The challenge of equipment design will be to identify the forces and perform stress calculations on the most critical locations. These critical locations are situated at the connections between kneading elements and shaft and housing, the shaft tube connection to the drive, the shaft deflection and bearing forces. A batch test can be performed and the torque behavior characterized. The scale-up to a continuous system is relatively simple (although of mechanical complex design) since the torque fluctuation will essentially be the same, because it is limited to a small fraction of the shaft length.

The situation becomes much more complex if the high torque zone is extended over a significant length of the kneader shaft. In order to be able to convey the product through the kneader, the kneading elements have to be mounted with a specific transport angle or pitch. The shaft development angle has to be equal or greater than this pitch in order to avoid transport blockage by the following disc row, but also to evenly distribute the torque forces over each shaft section over one shaft revolution. For each disc row there will be a different timing, when the torque peak occurs at a specific shaft turn angle. The sum of all these individual torque distributions will be the global shaft load. The problem is, that without knowledge of the torque behavior, the individual torque loads may superimpose (leading to enormous torque fluctuations) or interfere (which is desired).

Experimental

A concentrated rubber solution was fed to a single shaft continuous kneader of 5 m³ process volume. The rubber was devolatilized under vacuum and discharged at a certain higher temperature due to mechanical heat input. This kneader was equipped with a Hydraulic drive system (see figure 3). The shaft torque was monitored by measuring the pressure difference of the hydraulic oil fluid between motor inlet and outlet:

$$T_z = \mu d_{Shaft} \pi n + (p_{Hyd,in} - p_{Hyd,out}) t_{spec} \quad (1)$$

In parallel we monitored the shaft speed. These measurements were performed at a resolution of about 8 ms. The kneader had to be under continuous operating conditions. We can assume that this was the case because the equipment had run for 2 days under similar process conditions.

It appeared that the compressibility of the oil led to shaft speed fluctuations. Therefore the exact angle position during one shaft turn had to be calibrated using the speed measurement. In order to obtain a representative measurement sample, we overlaid the data of 5 shaft turns. No major deviations of the data between individual turns were observed.

The recorded data was then compared to our new model.

Results and discussion

In order to compare the measurement to our new torque distribution model, we needed to break down the measured global torque T_z into different torque levels over length induced by the process. This torque distribution over the length was determined by an already existing process scale-up program (1). This program calculates the mechanical heat input by shear and the contact heat as function of jacket and product temperature, the shaft speed and the local product fill level. The fill level was calculated using an already existing kneader transport model for this kneader type.

The simulation program uses a differential approach and integrates the torque level over the length. For the evaluation of the torque level over the length and the shaft angle, the amount of information needed to be condensed. We chose to divide the torque into an amount of individual interactions equal to the amount of kneading elements (about 40) and integrated the torque level over each section. The result was a length vector of 40 rows and its corresponding torque level vector.

The next step was to break down each torque level into individual interactions between the shaft, the product and the static parts of the equipment (counterhooks and housing). These individual torque levels can be calculated knowing the induced interaction forces and the level. We can distinguish between 2 types of forces in a kneader reactor, shear forces and drag forces (2):

1. Shear Forces

Shear forces: product is extruded between kneading bars and an extended surface, which can be the kneader housing, the shaft or the disc elements welded on the shaft. These forces can be calculated by assuming a linear product velocity profile between the rotating (moving) part and the static part, thus a defined shear rate:

$$\tau_{shear} = \eta \left(\dot{\gamma} \right) \dot{\gamma} = \eta \left(\dot{\gamma} \right) \frac{v_{rel}}{\delta} \quad (2)$$

The shear tension has to be transformed to the corresponding force using the applicable surface on which it acts. This surface is delimited by (or defined by) the shear gap length and the channel depth.

Shear forces are generally constant over the shaft turn, but there are some exceptions because the shear surface may be interrupted. This is the case on kneader's discs and the kneader dome through holes used for vapor disengagement.

2. Drag Forces

Drag forces are induced when kneader elements force their way through the product mass. These forces become significant as soon as there is a relative speed between the product and the kneader elements. Generally, this is the case when static and dynamic kneader elements approach each other each pushing a certain amount of product. Since the product is highly viscous, there is laminar flow and wall effects are minor. Once two elements are close enough, the remaining gap fills up with product and the product cannot be pushed ahead of the kneading element any longer. It has to flow through gaps between the elements on the backside inducing an equal force on static and dynamic elements. This force is calculated using general fluid dynamic:

$$Eu = \frac{const}{Re} \quad (3)$$

where the constant has to be determined empirically or using an advanced fluid dynamics model. The exact moment, when the drag force starts to become significant is a direct function of how much product is accumulated before one individual kneading element. There is an obvious relationship between local fill level and this amount of product, but it has to be considered that the product can distribute itself on different elements closer or

farther away from the shaft tube. Another important aspect is that the angle between the two counterhook rows is not 180°, thus the forces induced by each row are not equal, since the configuration is not symmetric.

3. Shaft Torque

Each of these individual forces acts at a defined shaft angle position relative to an arbitrarily chosen 0 position. There were a total of 7 forces supposed to be significant. One shaft rotation was split up into 256 locations and the 3 forces (in Cartesian coordinates, z being the shaft axis) and 3 torque levels are added up into a dyne matrix.

This resulting dyne matrix can be used to calculate the global shaft torque induced by the process, but also of the flex torque and bearing forces. The global shaft torque at the connection of the motor to the shaft is the torque induced by the process and by the inertia of shaft and motor:

$$T_z = T_{z,process} + I \ddot{\varphi} = T_{z,process} + I 2\pi \frac{\partial n}{\partial t} \quad (4)$$

Figure 4 shows measurement and calculation both on the same graph. As we can see the location of the hydraulic pressure peaks correspond well. The gap between the measured and calculated torque level is around 5 to 10 %.

4. Shaft Speed fluctuations

The hydraulic system oil compressibility reacts to the torque fluctuation by changing the hydraulic fluid pressure ahead of the motor. Since between pump and motor there is always a certain amount of oil in the piping, this oil is compressed and reduces in volume. This happens at each torque peak. Since the volumetric oil flow at the pump outlet is constant (the pump is a volumetric piston pump), the oil flow at the motor can be expressed by the oil flow of the pump plus the fluctuation due to the compressed oil in the connection line. The shaft speed can be expressed as a function of the hydraulic pressure ahead of the motor:

$$n = \frac{n_{av}}{1 + \frac{V_{line}}{V_{motor}} \varepsilon_{Oil} \frac{\partial p_{Hyd,in}}{\partial \varphi} 2\pi} \quad (5)$$

This expression allows calculation of the shaft speed as function of the shaft angle and pressure fluctuation. Figure 5 shows a plot of calculated rpm data compared to measured rpm.

Since we had calculated the torque generated by the process, we can now calculate the shaft speed at any specific shaft angle using the torque data of the process model. This requires a loop calculation of eq. 1, 4 and 5. According to eq. 4 the shaft speed fluctuation can either

- Smooth the torque fluctuations, which means a higher shaft torque is possible without damaging the drive

end connection to the motor. Note that if the process torque is monitored using the hydraulic drive system (acc. to eq. 1), there will be a gap between the measured torque and that generated by the process. Critical parts in the process chamber should have enough reserve to cope with these non-monitored forces.

- Or accelerate the process-generated torque fluctuations. This is safer for the process parts because torque peaks can be cut off by a pressure relief valve on the hydraulic system. However, the kneader product capacity may be reduced.

Figure 6 shows the calculated shaft speed fluctuation from the calculated hydraulic pressure generated by the process torque. Obviously, the errors of both calculations add up, which means that this calculation is the lowest in accuracy of this paper. Still the result shows a good representation when the peaks occur and which level to be expected.

Summary

A comprehensive calculation of torque fluctuations on industrial kneader equipment was presented. Using an existing process model, we could calculate these fluctuations depending on the kneader geometry and rheological behavior of the processed product. The response of the hydraulic drive system to these fluctuations could be assessed. The calculation will allow proper definition of the optimal kneader geometry for processing highly viscous fluids.

Nomenclature

d	diameter
n	shaft speed in rps
p	pressure
t _{spec}	specific torque
t	time
v	product velocity
Eu	Euler number
I	Inertia
Re	Reynolds number
T	torque
V _{line}	Oil volume in line to motor
V _{motor}	displaced oil volume of motor per shaft turn
δ	gap width
η	viscosity
μ	seal friction

•	
$\dot{\gamma}$	shear rate
ε	compressibility
φ	shaft angle
τ	tension

indices:

av	average
Hyd	hydraulic
line	hydraulic oil feed line to motor
rel	relativ
x,y,z	Cartesian coordinates, z in shaft length direction

References

1. Daniel Witte, Computer Scale-Up Model For Desolventizing Highly Viscous Polymers In Kneader Equipment, Antec (2005)
2. Diploma work D.Jermann/T.Lukic "Newton-Reynoldszahl für LIST-Kneter", Fachhochschule beider Basel (FHBB), 2003

Key Words

Torque, shaft speed, modeling, kneader, high viscosity, fluctuation

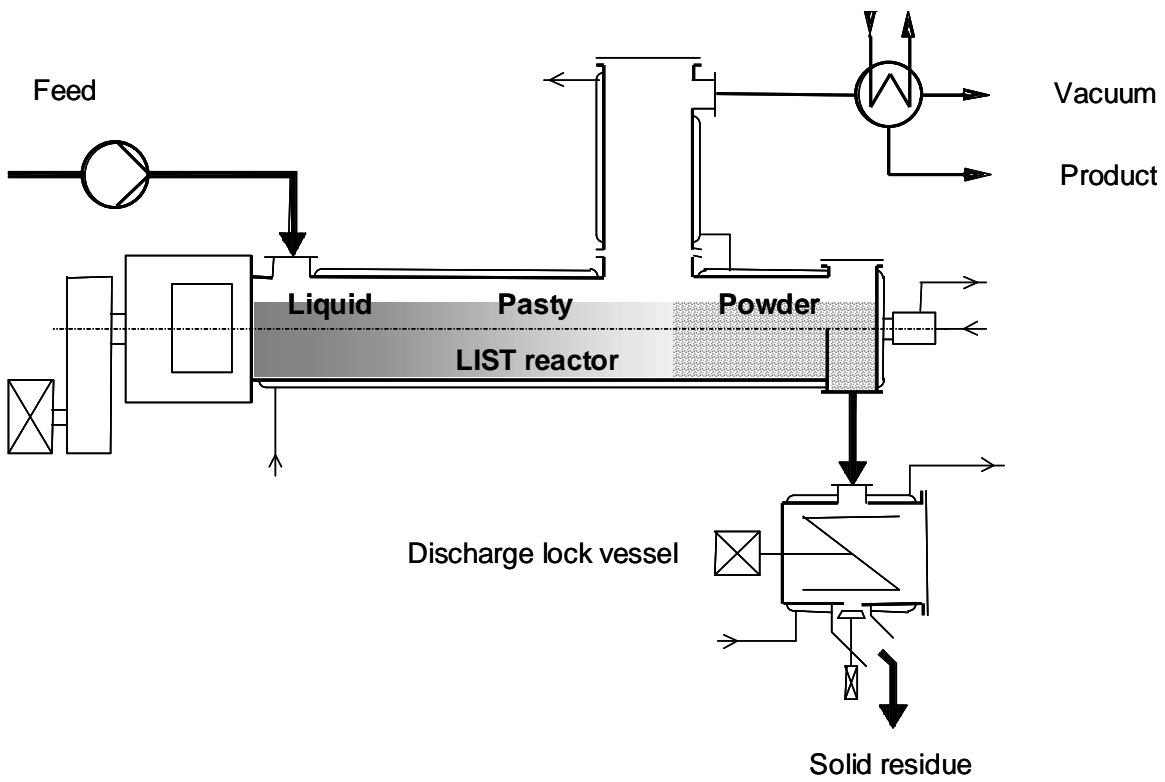


Figure 1: Typical kneader process

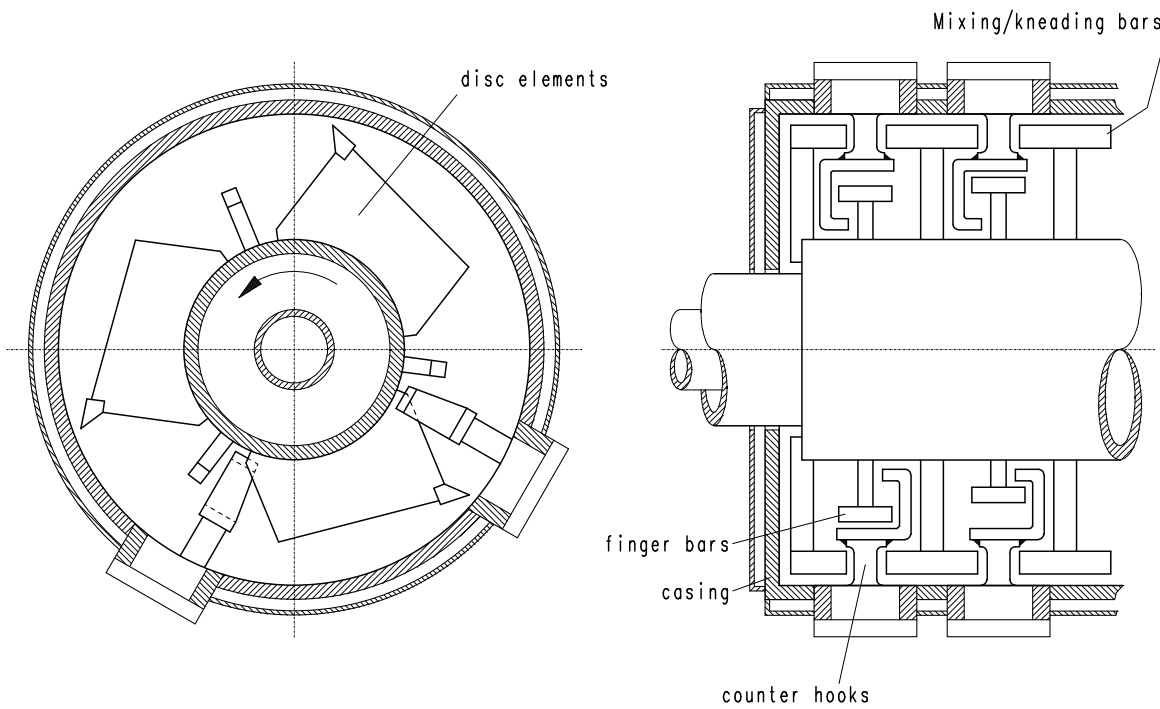


Figure 2: Single shaft kneader

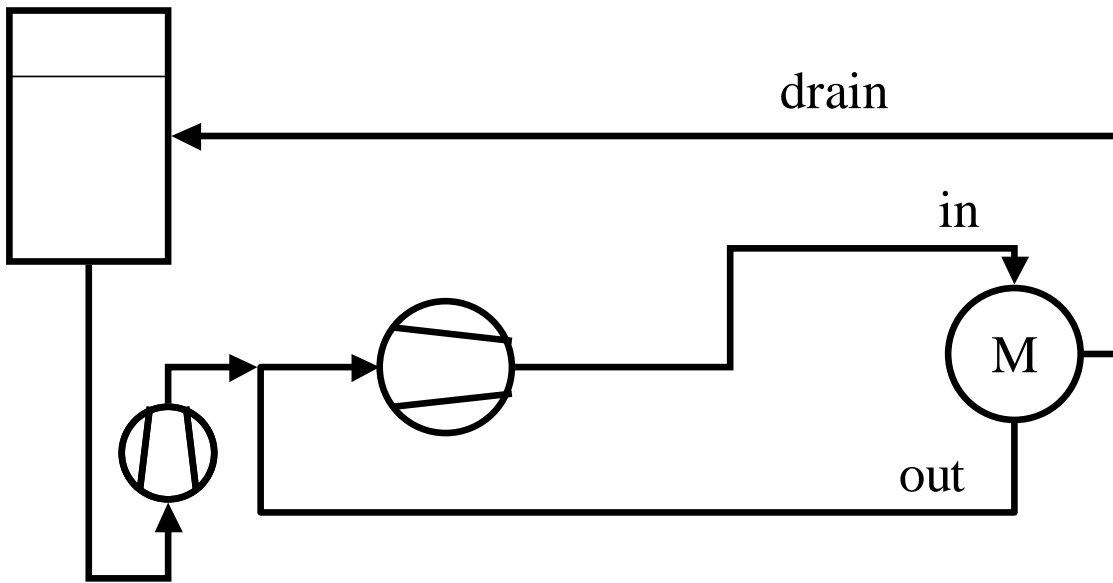


Figure 3: Hydraulic drive system

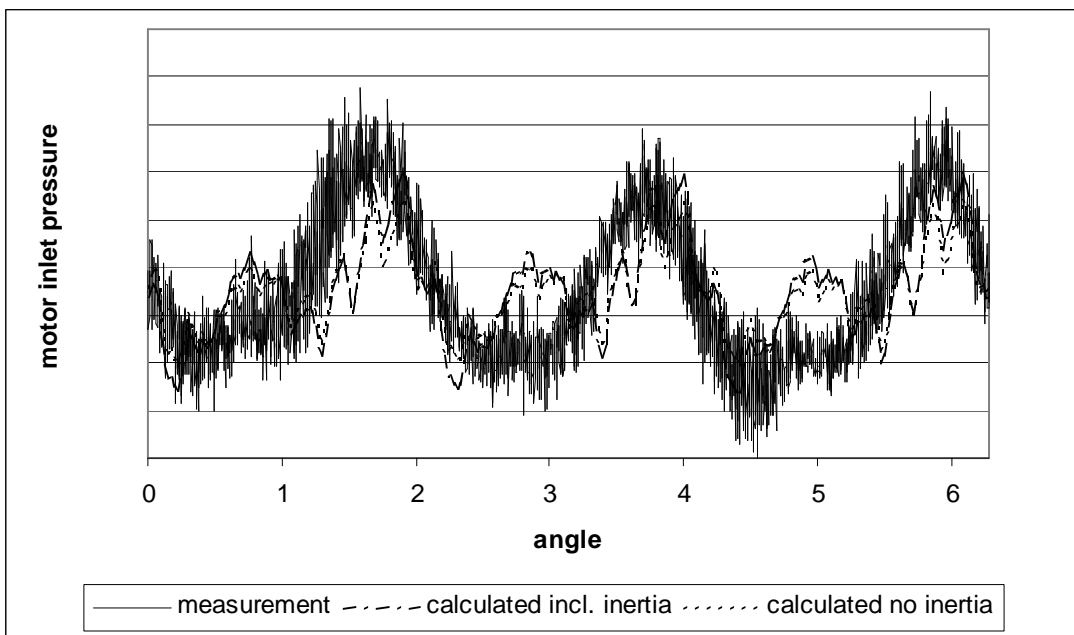


Figure 4: Hydraulic pressure before motor inlet

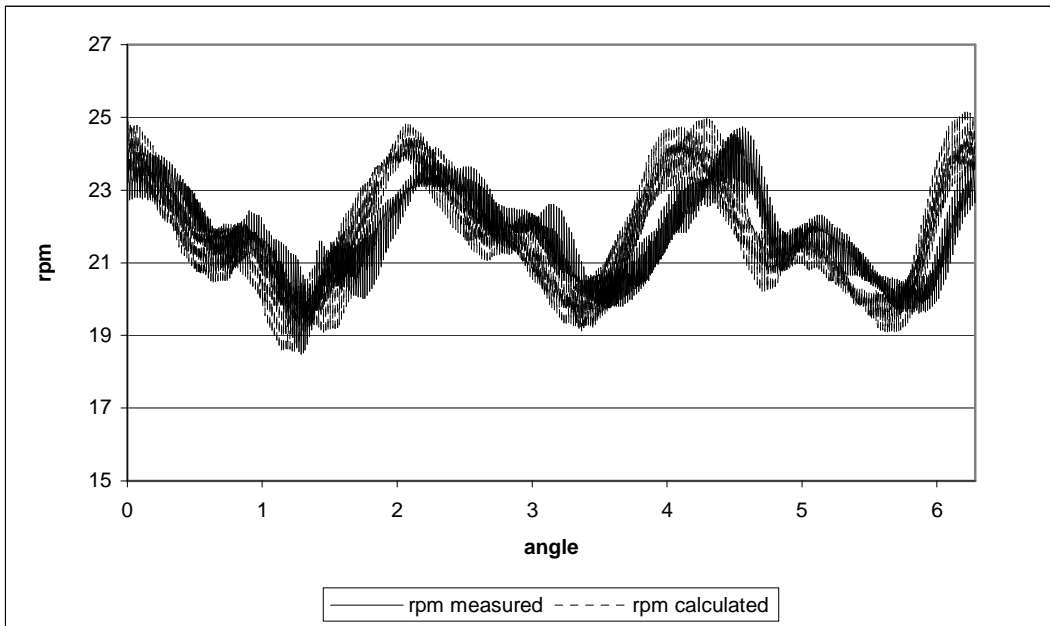


Figure 5: Shaft speed calculated from measured hydraulic pressure

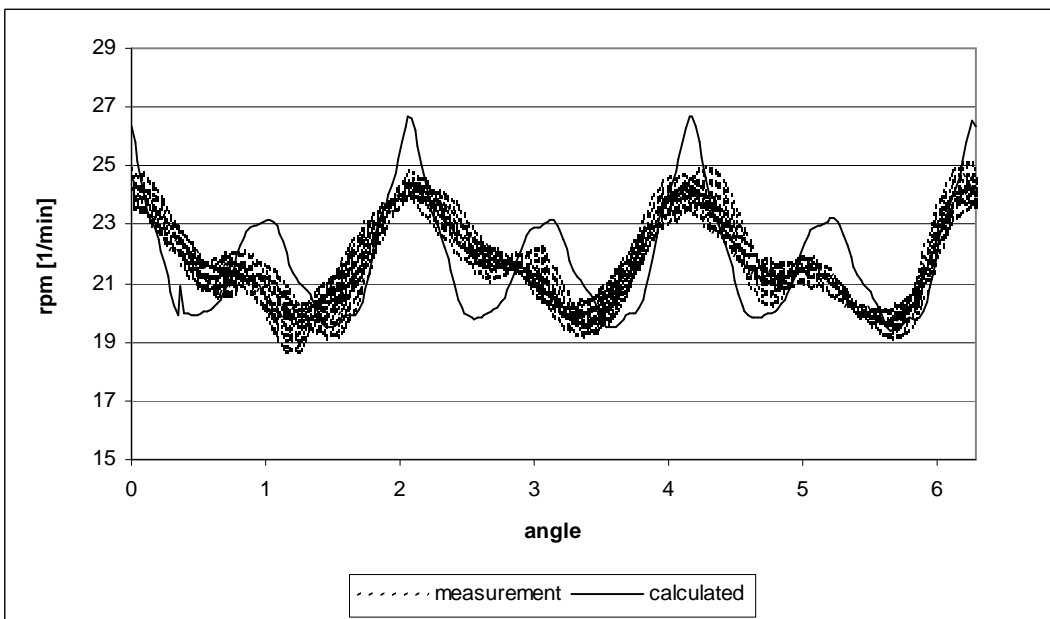


Figure 6: Shaft speed calculated from calculated torque